Transport properties in $FeSe_{0.5}Te_{0.5}$ nanobridges

C. H. Wu,[1,2,a)] W. C. Chang,[1] J. T. Jeng,[3] M. J. Wang,[4] Y. S. Li,[5] H. H. Chang,[4] and M. K. Wu[5]

[1]*Department of Physics, National Chung-Hsing University, Taichung 402, Taiwan*
[2]*Institute of Nanoscience, National Chung-Hsing University, Taichung 402, Taiwan*
[3]*Department of Mechanical Engineering, National Kaohsiung University of Applied Sciences, Kaohsiung 807, Taiwan*
[4]*Institute of Astronomy and Astrophysics, Academia Sinica, Taipei, Taiwan*
[5]*Institute of Physics, Academia Sinica, Taipei, Taiwan*

(Received 6 March 2013; accepted 23 May 2013; published online 6 June 2013)

FeSeTe nanobridges of different widths have been fabricated on MgO substrates using focused ion beams. These nanobridges exhibit the Josephson effects. The current-voltage curves of junctions with 248–564 nm wide follow the resistively and capacitatively shunted junction model. Shapiro steps under microwave radiation were clearly observed in these nanobridges. The products of the critical current and normal state resistance (I_cR_n) are remarkably high. The temperature dependence of I_cR_n product followed the Ambegaokar-Baratoff (A-B) relation. The value of energy gap of FeSeTe calculated from the A-B relation is $3.5k_BT_c$. The nanobridge junctions have a strong potential for high frequency applications. © *2013 AIP Publishing LLC*.
[http://dx.doi.org/10.1063/1.4809920]

The iron-based superconductors have been extensively investigated since their discovery became a surprise to the superconductivity research community.[1–8] Josephson effects and their applications in iron-based superconductors were also reported.[1,2] However, certain properties of various iron-based superconductors have yet to be elucidated, such as the coupling mechanisms of Cooper pairs in iron-based superconductors. Planar Josephson junctions of iron-based superconductors have also not been widely investigated. To date, only two types of Josephson junctions of Fe-based superconductor thin films have been studied. One was fabricated with a bicrystal grain boundary,[3] and the other used an superconductor–normal metal–superconductor (SNS) structure of $BaFe_2As_2$:Co thin film.[4] Shapiro steps were clearly observed with those junctions, indicating the possible application of such materials in Josephson devices. The magnetic field and temperature-dependence of J_c have been measured, and the structures of junctions have been observed with high-resolution transmission electron microscopy (HR-TEM), showing that the Josephson junctions of iron-based superconductors behave like the SNS junctions.

In this study, the transport properties, Josephson effects, and energy gaps of FeSeTe nanobridges made by focused ion beams (FIB) are investigated.

The properties of bulk $FeSe_xTe_{1-x}$ have been studied.[5–8] The superconductivity in $FeSe_xTe_{1-x}$ (FeSeTe) varies with x, and the critical temperature is highest when x equals 0.5. High quality FeSeTe thin films are typically deposited by Pulsed Laser Deposition (PLD). The critical temperature depends on the film thickness and the substrate material.[9] In this work, the FeSeTe thin film with a thickness of 100 nm on a MgO substrate is also prepared by PLD. The grown FeSeTe thin film has favorable superconducting properties with a critical temperature T_c of 14.6 K. To protect the thin films and to increase the accuracy in dimensions of junctions, a gold layer is deposited by a DC sputtering system on top of the FeTeSe thin film before the FIB process. The Au layer also provides low contact resistance and high conductivity on the surface of the FeSeTe thin film. To form the junction, FeSeTe bridges with a width of 8 μm are constructed by standard photolithography and Ar ion milling, and the nanobridges of a width less than 1 μm are subsequently formed via FIB etching. The electrical properties are measured using a four-probe technique.

Figure 1 presents a scanning electron microscopic (SEM) image of the nanobridges with a width of 564 nm. To reduce the damage caused by containment of gallium ions, the dwell time and passes of ion beam were optimized during the FIB machining process.

Figure 2 shows the voltage-current (V–I) characteristic and the fit curve to the resistively and capacitatively shunted-junction (RCSJ) model for the nanobridge of

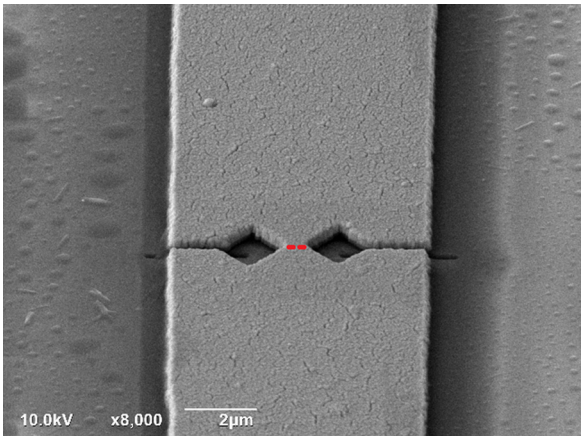

FIG. 1. SEM images of a FeSeTe nanobridge fabricated by FIB.

[a)]Author to whom correspondence should be addressed. Electronic mail: chwu@phys.nchu.edu.tw. Phone: 886-4-22840427. Fax: 886-4-22862534.

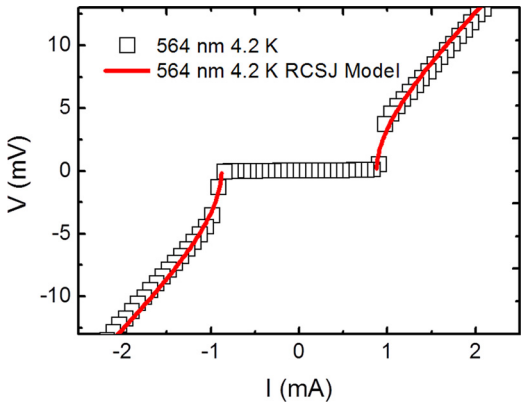

FIG. 2. *V–I* characteristics of 564 nm wide nanobridges at T = 4.2 K and fitted by RCSJ-model.

564 nm width. By using the RCSJ model, the current passing through the junction is[10]

$$I = C\frac{dV}{dt} + GV + I_c \sin\varphi, \tag{1}$$

where C denotes the capacitance, G is the conductance, and I_c is the Josephson supercurrent. The McCumber parameter, $\beta_c = 2\pi I_c{}^2 R^2 C/\Phi_0$,[10] is found to be less than 0.65, where R and C are, respectively, the normal resistance and equivalent capacitance of the junction, while Φ_0 is the flux quantum. All of the *V–I* characteristics of nanobridges with different widths were found to agree closely with the RSCJ-model.

Over the past few decades, FIB-milled nanobridge junctions made of various superconductors, e.g., YBCO, Nb, and MgB_2, have been reported. However, with our device, Shapiro steps are observed when 248–564 nm wide nanobridges are irradiated with microwaves. Figure 3 shows that the microwave irradiation suppresses I_c, and Shapiro steps are observed when a 564 nm wide nanobridge is irradiated with microwaves at 7.8 GHz. The step height is found to be 16 μV, in agreement with the relation $V = hf/2e$, where h is the Plank's constant and e is the elementary charge. The *V–I* characteristics of the FeSeTe nanobridges herein are similar to those of the Fe-based bicrystal junctions,[3] the magnitude of the critical current is approximately

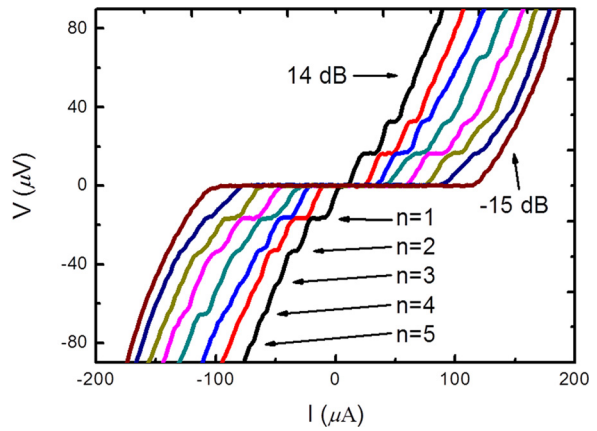

FIG. 3. The *V–I* characteristics of 564 nm wide nanobridges at T = 11 K. The Shapiro steps irradiated by the microwave of frequency 7.8 GHz. The microwave power ranges from −15 to 14 dB.

TABLE I. The parameter of RCSJ-model.

Width of nanobridges	I_c[a] (μA)	R_n[b]	I_{ex}[c] (μA)	β_c[d]	C[e] (pF)
248 nm, T = 4.2 K	380	7.0			
384 nm, T = 4.2 K	660	5.4			
564 nm, T = 4.2 K	880	6.8	40	0.3	2.7
672 nm, T = 4.2 K	1380	6.2	130	0.65	2.9

[a]I_c is the critical current of nanobridges.
[b]R_n is the normal resistance of nanobridges.
[c]I_{ex} is the excess current of nanobridges.
[d]β_c is the McCumber β_c of nanobridges.
[e]C is the capacitance of nanobridges.

1 mA with a small excess current, and *V-I* characteristics have minor or no hysteresis. We believe that some grain boundaries in the nanobridges are responsible for the weak link behavior. The nanobridges of 150 nm width have been fabricated, but the critical currents are very small, and Shapiro steps cannot be observed.

Table I presents the values of I_c, R_n, and β_c obtained from the *V–I* characteristics of nanobridges fitted by the RCSJ model. The values of I_c and I_{ex} increase with the width of the nanobridge. The R_n, which ranges from 5.2 to 7.0 Ω, and β_c also depends on the width. The β_c of 672 nm wide nanobridge is 0.65. A capacitance of 2.9 pF was derived using the McCumber equation. This is larger than the capacitances of the other nanobridges (with widths 564 nm, 384 nm, and 248 nm).

The value of β_c for the 564 nm wide nanobridge is 0.3, and the *V–I* curve exhibits slight hysteresis. At T = 4.2 K, the critical current I_c is 880 μA with an excess current of ~40 μA, and the normal resistance is 6.8 Ω. The I_cR_n product is approximately 6.0 mV. The value of I_cR_n is quite large, as it is for other superconducting materials, such as the MgB_2 break junction.[11] The β_c values of nanobridges with widths of less than 564 nm are small, and the nanobridge with a width of 384 nm is negligibly small and not observable.

Figure 4 plots the *V–I* and *dV/dI*-versus-*I* characteristics of the 564 nm wide FeSeTe nanobridge at temperatures from 12.3 K to 4.2 K. The critical temperature and the critical current are, respectively, 12.3 K and 100 μA. The critical currents of 835 μA and 880 μA correspond to temperatures of

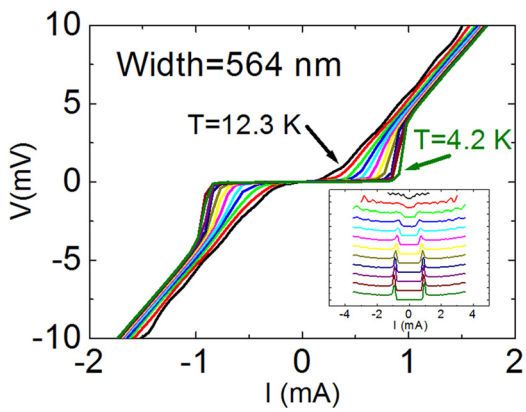

FIG. 4. *V–I* characteristic of 564 nm nanobridges at different temperatures. The inset shows the *dV/dI*-I curves. The small change in critical current of the nanobridges observed when $T < T_c/2$.

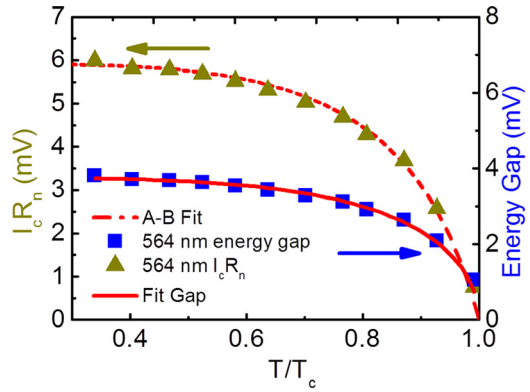

FIG. 5. The temperature dependence of I_cR_n product (triangle) and superconducting energy gap (rectangle) of the 564 nm wide nanobridge.

6.5 K and 4.2 K, and the critical current at 3.9 K is close to 880 μA. The small change in critical current of the nanobridge was observed when the temperature is below 6.5 K, which is about half of the critical temperature ($T_c = 12.6$ K).

Figure 5 plots the temperature-dependence of the I_cR_n product. The relationship between temperature and I_cR_n is found to follow the Ambegaokar-Baratoff relation[12]

$$I_cR_n = \frac{\pi}{2}\frac{\Delta(T)}{e}\tanh\left(\frac{\Delta(T)}{2k_BT}\right), \quad (2)$$

where e is the elementary electric charge, $\Delta(T)$ is the temperature-dependent superconducting energy gap, and k_B is the Boltzmann constant. Generally, the A-B relation is used to describe tunneling Josephson junctions exhibiting stable superconducting properties at temperatures below $T_c/2$ with a large R_n and I_cR_n product, which is promising for SQUID and high frequency applications. Since the magnitude of the peak-to-peak (V_{pp}) voltage of SQUID is positively correlated with the normal resistance (R_n), it is interesting to verify the properties of the SQUID comprising such junctions. The high frequency sensor can be fabricated using Josephson junctions with large I_cR_n products, when a junction is irradiated with microwaves at 0.1 THz, the Shapiro step height is 207 μV, in agreement with the relation $V = hf/2e$.

From past experience, the temperature-dependence of the critical current in YBCO, MgB_2, and BaFeAs:Co nanobridges fabricated by FIB is similar to that of the bicrystal junction, and it reveals *SNS* behavior. For the SNS and bicrystal junctions, the critical current increases as the temperature decreases in proportion to $1\text{-}(T/T_c)^{\alpha}$, where $\alpha = 1$ or 2 (at high temperatures). However, the data obtained in the current study differ from those obtained for a bicrystal and SNS junction.

The solid line in Fig. 5 shows the superconducting energy gap of the FeSeTe nanobridge that was calculated from the A-B relation. The curve of the fitted energy gap as a function of temperature is consistent with the energy gap of the BCS-type temperature dependence.[13] However, this superconducting energy gap, which did not match the experimental, was calculated using the formula of the SNS-long junction and the I_cR_n product at various temperatures

$$I_c(T;L) = \frac{2}{\pi eR_n}\frac{|\Delta(T)|^2}{k_BT_c}\frac{L/\xi}{\sinh(L/\xi)}, \quad (3)$$

where L is the barrier thickness of the junction and ξ is coherence length of the thin film. The value of $\Delta(0)$ for the $FeSe_{0.5}Te_{0.5}$ nanobridges of 564 nm width is 3.5 k_BT_c.

Superconducting energy gaps of $FeSe_xTe_{1-x}$ can be determined using various methods. For example, the energy gap of the heterojunction is estimated to be 2.06 meV,[14] but an energy gap of 2.3 meV is measured by STM.[15] Accordingly, the calculated $2\triangle/k_BT_c$ is 3.8, which is close to the value based on BCS theory. The point-contact Andreev reflection (PCAR) method, in which the energy gap is calculated from dI/dV, reveals strong coupling superconductivity in the $FeTe_{0.55}Se_{0.45}$ thin film. The energy gap is 3.8 meV at 1.7 K. The superconducting energy gaps that were calculated with the I_cR_n products agree with that calculated using the PCAR method.[16] Our data are similar to that of FeSeTe break junctions, which were investigated by Park.[16]

In summary, FeSeTe nanobridges were fabricated with widths from 248 to 672 nm on MgO substrates using a FIB. The current-voltage characteristics reveal that the critical currents of the nanobridges increase as the temperatures decreases, but the variation in the critical current is small and below $0.5T_c$. The V-I characteristics can be fitted by the RCSJ-model with a small excess current and a slight hysteresis, whereas the temperature-dependence of critical current can be fitted by the Ambegaokar-Baratoff relation. The superconducting energy gap of the FeSeTe nanobridges is $3.5k_BT_c$. The effect of microwave irradiation on the junctions is clearly observed. Further work to investigate the techniques for trimming the parameters of FIB FeSeTe junctions would be valuable for device applications.

[1]P. Seidel, Supercond. Sci. Technol. **24**, 043001 (2011).
[2]K. Tanabe and H. Hosono, Jpn. J. Appl. Phys. **51**, 010005 (2012).
[3]T. Katase, Y. Ishimaru, A. Tsukamoto, H. Hiramatsu, T. Kamiya, K. Tanabe, and H. Hosono, Nat. Commun. **2**, 409 (2011).
[4]S. Döring, S. Schmidt, F. Schmidl, V. Tympel, S. Haindl, F. Kurth, K. Iida, I. Mönch, B. Holzapfel, and P. Seidel, Supercond. Sci. Technol. **25**, 084020 (2012).
[5]B. C. Sales, A. S. Sefat, M. A. McGuire, R. Y. Jin, and D. Mandrus, Phys. Rev. B. **79**, 094521 (2009).
[6]S. Li, C. Cruz, Q. Huang, Y. Chen, J. W. Lynn, J. Hu, Y. L. Huang, F. C. Hsu, K. W. Yeh, M. K. Wu, and P. Dai, Phys. Rev. B **79**, 054503 (2009).
[7]C. L. Huang, C. C. Chou, K. F. Tseng, Y. L. Huang, F. C. Hsu, K. W. Yeh, M. K. Wu, and H. D. Yang, J. Phys. Soc. Jpn. **78**, 084710 (2009).
[8]K. W. Yeh, C. T. Ke, T. W. Huang, T. K. Chen, Y. L. Huang, P. M. Wu, and M. K. Wu, Cryst. Growth Des. **9**, 4847 (2009).
[9]T. Yoshimoto, Y. Ichino, Y. Yoshida, T. Kiss, M. Inoue, K. Matsumoto, A. Ichinose, H. Kai, R. Teranishi, N. Mori, and M. Mukaida, J. Phys. Conf. Ser. **234**, 012051 (2010).
[10]A. Barone and G. Paternó, *Physics and Applications of the Josephson Effect* (Wiley, New York, 1982).
[11]R. S. Gonnelli, A. Calzolari, D. Daghero, and G. A. Ummarino, Phys. Rev. Lett. **87**, 097001 (2001).
[12]V. Ambegaokar and A. Baratoff, Phys. Rev. Lett. **10**, 486 (1963).
[13]K. Senapati, M. G. Blamire, and Z. H. Barber, Nat. Mater. **10**, 849 (2011).
[14]C. T. Wu, H. H. Chang, J. Y. Luo, T. J. Chen, F. C. Hsu, T. K. Chen, M. J. Wang, and M. K. Wu, Appl. Phys. Lett. **96**, 122506 (2010).
[15]T. Kato, Y. Mizuguchi, H. Nakamura, T. Machida, H. Sakata, and Y. Takano, Phys. Rev. B **80**, 180507 (2009).
[16]W. K. Park, C. R. Hunt, H. Z. Arham, Z. J. Xu, J. S. Wen, Z. W. Lin, Q. Li, G. D. Gu, and L. H. Greene, e-print arXiv:1005.0190v1.